RDF investigations on concentrated solutions of poly(*p*-phenylene-1,3,4-oxadiazole) in sulphuric acid

D. Hofmann, P. Weigel, J. Ganster and H.-P. Fink
Institute of Polymer Chemistry 'Erich Correns', Academy of Sciences of the GDR, 1530 Teltow-Seehof, Kanstrasse 55, GDR
(Received 7 November 1989; accepted 12 February 1990)

Reduced radial distribution functions (RDFs) for non-crystalline solutions of poly(*p*-phenylene-1,3,4-oxadiazole) (POD) in H_2SO_4 have been determined and discussed for the first time. In solutions of up to 14 wt% POD in H_2SO_4 the POD monomeric units act as simple perturbations of the correlation lattice of the pure solvent. Between 14 and 15 wt% POD content a phase transition from isotropic solution to crystal solvates and H_2SO_4 occurs. The short range interactions of POD molecules with the correlation lattice of a 96.2 wt% aqueous H_2SO_4 solvent are considerably stronger than for the same POD content in a 100% H_2SO_4 solvent.

(Keywords: poly(*p*-phenylene-1,3,4-oxadiazole); sulphuric acid; wide-angle X-ray scattering; radial distribution function)

INTRODUCTION

Fibres with high thermal stability can be spun from solutions of poly(*p*-phenylene-1,3,4-oxadiazole) (POD) in sulphuric acid[1–4]. The characterization of the internal structure of these solutions is especially important because POD molecules are semi-rigid in H_2SO_4. Up to now, POD solutions in sulphuric acid have been investigated using, for example, polarized light microscopy, viscosimetry, nuclear magnetic resonance spectroscopy and transmission electron microscopy[5–8]. The usual wide angle X-ray scattering (WAXS) studies have been also performed, but mainly to characterize crystal solvates which are present in POD solutions of higher concentration[8–10]. In this paper we will discuss reduced radial distribution functions (RDFs) for the first time for non-crystalline solutions of POD in 100 and 96.2 wt% aqueous H_2SO_4 solvents.

Weidner *et al.*[11,12] investigated the intramolecular RDF and reduced intermolecular RDF of liquid 100% sulphuric acid at 293 K. The short range order was described by a correlation lattice. Two possible monoclinic base centred unit cells belonging to the space groups C2/c and C2 were determined. In liquid 100% H_2SO_4 the molecules were found to be preferentially arranged in layers parallel to the base of the unit cell. The occupancy of the molecular sites in the unit cell was determined to be 85%. Within a layer, the molecules were assumed to be netted by hydrogen bonds with a length of ≈ 0.255 nm. Since the investigation of Weidner *et al.* was very careful, we used the 100% RDF given by them as a standard. In the present paper the influence of different POD contents in 100 and 96.2 wt% aqueous H_2SO_4 solvents on the reduced RDF will be discussed.

EXPERIMENTAL

Samples

The following samples were investigated:

Sample 1: 100% H_2SO_4;
Sample 2: 5 wt% POD in 100% H_2SO_4;
Sample 3: 10 wt% POD in 100% H_2SO_4;
Sample 4: 14 wt% POD in 100% H_2SO_4;
Sample 5: 15 wt% POD in 100% H_2SO_4;
Sample 6: 96.2 wt% H_2SO_4;
Sample 7: 0.5 wt% POD in 96.2 wt% H_2SO_4;
Sample 8: 6 wt% POD in 96.2 wt% H_2SO_4.

The solutions were placed between 0.08 mm thick PE foils, which were welded together to ensure exclusion of humidity.

WAXS measurements

The experiments were performed at 293 ± 1 K in symmetric transmission mode on a horizontal X-ray counter diffractometer HZG3 (Freiberger Präzisionsmechanik, GDR) using MoK_α radiation. A LiF monochromator in the primary beam was used and the scattered intensity was recorded in the angular range $2° \leqslant 2\theta \leqslant 120°$ ($\Delta 2\theta = 0.6°$) with a NaI scintillation counter and an impulse height analyser. Four scans were made for every sample to eliminate slowly varying experimental conditions. The minimum number of counts was $\approx 10^5$.

Data processing

In the first stage the data were corrected for background, polarization and absorption using the formula:

$$I_{corr}(\theta_i) = \frac{I_{meas}(\theta_i) - I_{back}(\theta_i)\exp(-\mu t/\cos\theta_i)}{1 + 1.8706\cos^2\theta_i(\cos 2\theta_i - 1)} \times \exp((\mu t + \delta t')/\cos\theta_i)\cos\theta_i \quad (1)$$

where:
$I_{corr}(\theta_i)$ = corrected intensity;
$I_{meas}(\theta_i)$ = measured intensity;
$I_{back}(\theta_i)$ = background (air and PE sample holder foils scattering) intensity normalized to the actual primary beam intensity;

0032-3861/91/0200284-06

μ = linear absorption coefficient of the sample;
δ = linear absorption coefficient of the PE sample holder foils;
t = sample thickness;
t' = thickness of sample holder foils;
1.8706 = constant depending on the monochromator Bragg angle used (here 10.202°).

In the second stage a parabolic extrapolation of the $I_{corr}(\theta)$ curve to $\theta = 0°$ was performed followed by correction for multiple scattering. For the latter the following approximate correction formula based on results of Monte Carlo simulations performed by Pitkänen *et al.*[13,14] was used:

$$I_{corr,m}(\theta_i) = I_{corr}(\theta_i)/(b\theta_i) \quad (2)$$

with

$$b = 0.310\mu t[\rho/(\text{g cm}^{-3})]^{\frac{1}{2}}/\theta_{max} \qquad \mu t < 0.25$$
$$0.0775[\rho/(\text{g cm}^{-3})]^{\frac{1}{2}}/\theta_{max} \qquad \mu t > 0.25$$

and ρ the density of the sample. In addition the I_{corr} values for $\theta_i > 26°$ were slightly smoothed (± 1 or ± 2 point averaging).

In the third stage the reduced interference function $i(s)$ was calculated as described in Reference 11 for pure H_2SO_4: $i(s) = [\alpha I_{corr,m}(s) - I_{coh}(s) - I_{incoh}(s)]/F(s)$, where $s = (4\pi/\lambda)\sin\theta$ and α is the scaling factor (to electron units) determined after Krogh-Moe[15]. $I_{coh}(s) = \sum_i f_i^2(s)$ is the coherent scattering intensity (where f_i is the atomic scattering factor[25] of the atom number i of the respective molecule) and I_{incoh} is the incoherent scattering intensity for one molecule of the sample (cf. atomic data of Reference 26). $F(s) = I_{coh}(s)/(\sum_i Z_i)^2$ is the sharpening function with Z_i the number of electrons for the ith atom of a molecule. (Note: for the POD solutions, $I_{coh}(s)$, $I_{incoh}(s)$ and $(\sum_i Z_i)^2$ were replaced by $\omega_{H_2SO_4} I_{coh}^{H_2SO_4}(s) + \omega_{H_2O} I_{coh}^{H_2O}(s) + \omega_{POD} I_{coh}^{POD}(s)$ and so on. $\omega_{H_2SO_4}$, ω_{H_2O}, ω_{POD} are the molecular fractions of H_2SO_4, H_2O and POD monomer units, respectively. Then the average molecule for $i(s)$ normalization is composed of

$$\omega_{H_2SO_4}(2H + S + 4O) + \omega_{H_2O}(2H + 1O) + \omega_{POD}(8C + 4H + 1O + 2N)$$

(see *Table 1*). *Figure 1* shows the $si(s)$ curves obtained in this manner for samples 1, 4, 6 and 8.

In the fourth stage the $si(s)$ curves were corrected for slowly varying systematic errors (e.g. errors in normalization and scattering factors). First, according to Kaplow *et al.*[16], the function $G(r)$ was obtained from $si(s)$ via a Fourier sine transform (FT) *for* $r = 0$–0.15 nm:

$$G(r) = (2/\pi)\int_0^{s_{max}} si(s)\sin(rs)\,ds \quad (3)$$

Table 1 Molecular fractions ω of H_2SO_4, H_2O and POD for samples 1–8

Sample	$\omega_{H_2SO_4}$	ω_{H_2O}	ω_{POD}
1	1	0	0
2	0.9654	0	0.0346
3	0.9297	0	0.0703
4	0.9003	0	0.0997
5	0.8928	0	0.1072
6	0.8230	0.1770	0
7	0.8203	0.1764	0.0033
8	0.7900	0.1700	0.0400

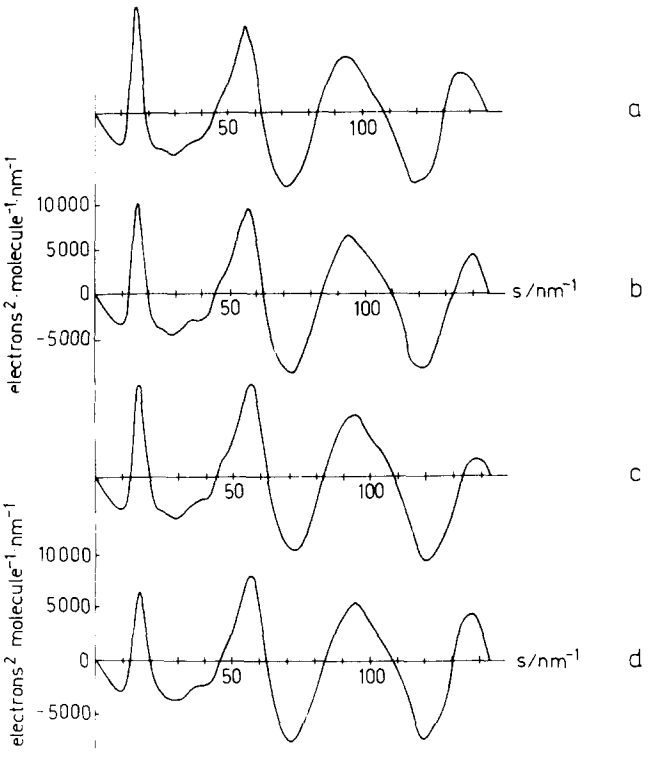

Figure 1 Reduced scattering intensity $si(s)$ for samples (a) 1, (b) 4, (c) 6 and (d) 8

The first physically relevant peak of this function is situated around $r \approx 0.14$ nm for the investigated samples, whereas peaks at lower r values are the result of systematic errors in $si(s)$ (the exception is the termination ripples of the first physically relevant peak). The course of an ideal $G(r)$ curve (i.e. $si(s)$ without systematic errors) below the small-r tail of the first physically relevant peak would be:

$$A(r) = -4\pi\rho_0 r\left[\omega_{H_2SO_4}\left(\sum_i Z_i^{H_2SO_4}\right)^2 + \omega_{H_2O}\left(\sum_i Z_i^{H_2O}\right)^2 + \omega_{POD}\left(\sum_i Z_i^{POD}\right)^2\right] \quad (4)$$

with ρ_0 the number density of average molecules (molecules nm^{-3}). Using this, a correction function

$$R(r) = G(r) - A(r) \quad (5)$$

($0 < r \lesssim 0.12$ nm as the beginning of the lower r tail of the first physically relevant peak) could be established and transformed giving

$$S(s) = \int_0^{r_{max}} R(r)\sin(rs)\,dr \quad (6)$$

Using $S(s)$, a first corrected $si(s)$ curve was obtained:

$$si(s)_{corr1} = si(s) - S(s) \quad (7)$$

$si(s)_{corr1}$ curves are shown in *Figure 2*.

A method originally proposed for pure sulphuric acid by Weidner *et al.*[11] was used as a second correction step for $si(s)$. For this at first the intramolecular reduced scattering intensity $si(s)_{intra}$ was calculated:

$$si(s)_{intra} = \omega_{H_2SO_4} si(s)_{intra}^{H_2SO_4} + \omega_{H_2O} si(s)_{intra}^{H_2O} + \omega_{POD} si(s)_{intra}^{POD} \quad (8)$$

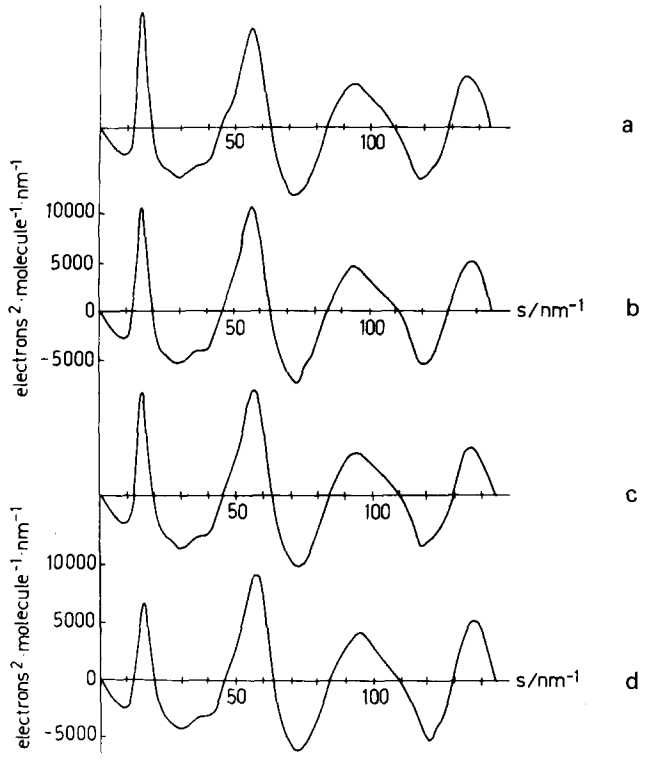

Figure 2 Reduced scattering intensity $si(s)_{corr1}$ after correction according to Reference 16 for samples (a) 1, (b) 4, (c) 6 and (d) 8

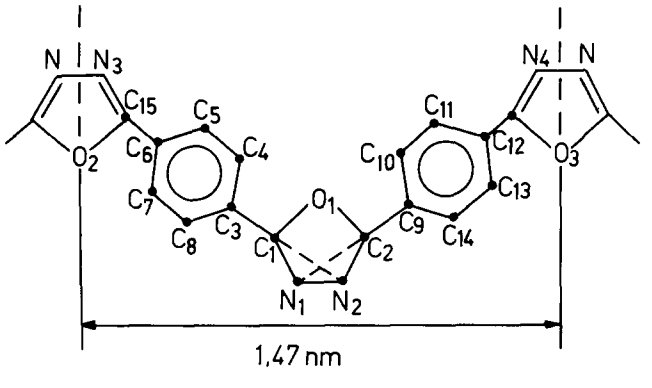

Figure 3 Molecular repeat unit for POD according to Reference 18

$i(s)^{H_2SO_4}_{intra}$, $i(s)^{H_2O}_{intra}$ and $i(s)^{POD}_{intra}$ were obtained via the Debye formula (see Reference 11). The atomic coordinates and the mean amplitudes of vibration for the atomic pairs for H_2SO_4 and H_2O were taken from References 12 and 17. The atomic coordinates for the POD molecular repeat unit (see *Figure 3*) were calculated from nearest neighbour distances and angular parameters given by Popik *et al.*[18] (see *Table 2* and Reference 19). It was assumed in this connection that $si(s)^{POD}_{intra}$ and $G(r)^{POD}_{intra}$ calculated from this repeat unit are representative of the whole POD molecule, at least for the $r \lesssim 0.24$ nm distances which are necessary for the intended $si(s)$ correction. The mean amplitudes of vibration were calculated as proposed in Reference 18. The intermolecular reduced scattering intensity $si(s)_{inter} = si(s)_{corr1} - si(s)_{intra}$ then contains remarkable peaks up to $s \approx 70\ nm^{-1}$ and only relatively small oscillations around the s-axis for $s > 70\ nm^{-1}$. This means that $G(r)_{inter} = FT[si(s)_{inter}]$ shows reduced termination ripples and is expected to reveal physically relevant peaks only for $r \gtrsim 0.24$ nm. (Note that hydrogen bonds are assumed to form the lowest relevant intermolecular distances of ≈ 0.26 nm in the given materials; see also Reference 12.)

Making use of these facts a similar procedure to that given in equations (4)–(6) but now with $r \lesssim 0.22$ nm was applied to give a correction function $S_2(s)$ and the final corrected $si(s)_{corr2} = si(s)_{corr1} - S_2(s)$ curve. (Note that the first correction step (4)–(6) was necessary, since otherwise $si(s)_{inter}$ would show erroneous oscillations that were too large in the $s > 70\ nm^{-1}$ range.) *Figure 4* shows $si(s)_{corr2}$ curves for samples 1, 4, 6 and 8.

Table 2 Atomic coordinates for the POD molecular repeat unit (see *Figure 3*) calculated using data given in Reference 18

Atom	x (nm)	y (nm)	z (nm)
C_1	−0.1041	0	0.0450
C_2	0.1041	0	0.0450
C_3	−0.2416	0	0.1046
C_4	−0.2718	0.0857	0.2110
C_5	−0.4002	0.0857	0.2665
C_6	−0.4984	0	0.2157
C_7	−0.4683	−0.0857	0.1093
C_8	−0.3399	−0.0857	0.0537
C_9	0.2416	0	0.1046
C_{10}	0.2718	−0.0857	0.2110
C_{11}	0.4002	−0.0857	0.2665
C_{12}	0.4984	0	0.2157
C_{13}	0.4683	0.0857	0.1093
C_{14}	0.3399	0.0857	0.0537
C_{15}	−0.6360	0	0.2752
C_{16}	0.6360	0	0.2752
O_1	0	0	0.1298
O_2	−0.7399	0	0.1903
O_3	0.7399	0	0.1903
N_1	−0.0705	0	−0.0647
N_2	0.0705	0	−0.0647
N_3	−0.6682	0	0.4019
N_4	0.6682	0	0.4019

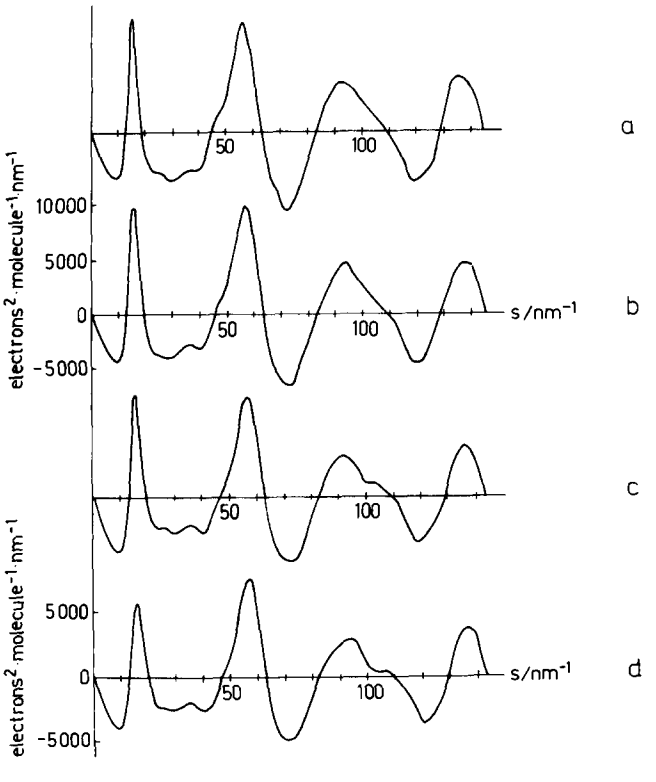

Figure 4 Reduced scattering intensity $si(s)_{corr2}$ after correction according to References 16 and 11 for samples (a) 1, (b) 4, (c) 6 and (d) 8

From $si(s)_{corr2}$, $G(r)$ was calculated using equation (3) with $i(s)$ replaced by $i(s)_{corr2}$. Termination errors were minimized by a special choice of sampling points for $G(r)$ according to Lovell *et al.*[20]. For that purpose the $si(s)_{corr2}$ curves were terminated at the node near 145 nm^{-1} and $G(r)$ was calculated at $r = n\pi/s_{max}$ $(n = 1, 2, \ldots)$. This treatment also retains the maximum possible resolution in $G(r)$, *which is equal to* π/s_{max}. Then the reduced RDF, $rG(r)$, was determined from the $G(r)$ values. These curves were smoothed for $r > 0.6$ nm to eliminate remaining errors due to termination. *Figures 5* and *6* show reduced RDFs obtained from $si(s)_{corr1}$ and $si(s)_{corr2}$ functions, respectively.

RESULTS AND DISCUSSION

The radial distribution function RDF(r) gives the number of electrons between the spherical shells of radii r and $r + dr$ with respect to an arbitrary atom placed at the origin[21]. For systems containing only one molecular

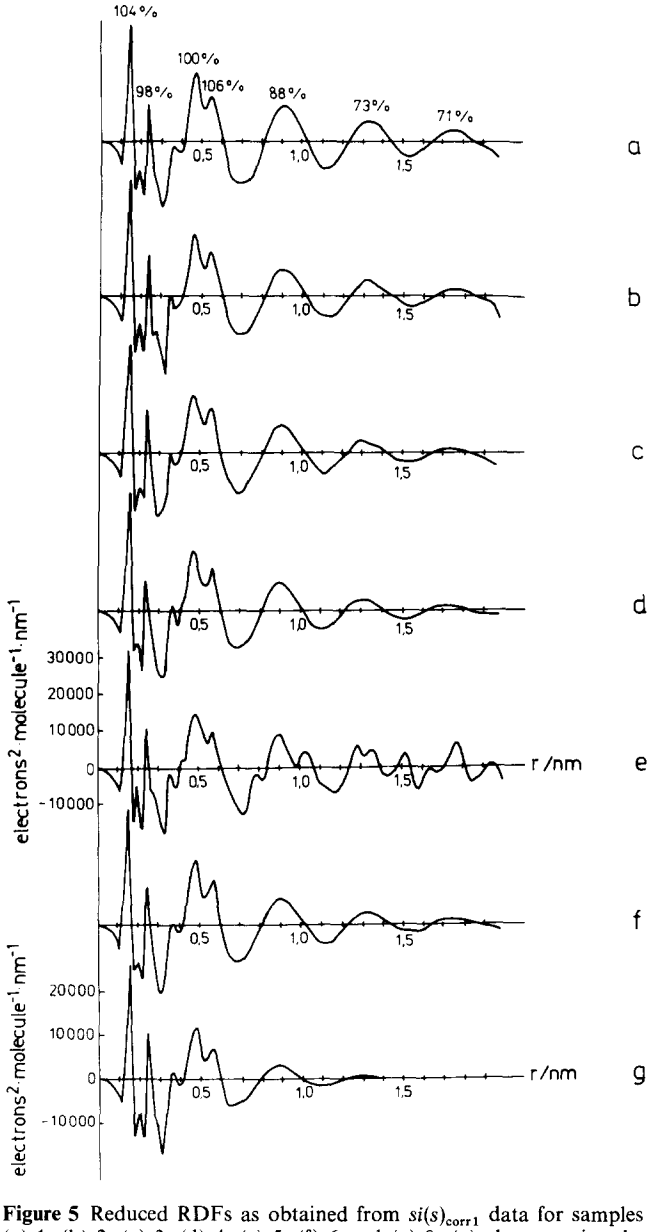

Figure 5 Reduced RDFs as obtained from $si(s)_{corr1}$ data for samples (a) 1, (b) 2, (c) 3, (d) 4, (e) 5, (f) 6 and (g) 8; (a) also contains the percentage ratios of the reduced RDF peak maximum heights of sample 1 to the corresponding data given in Reference 12

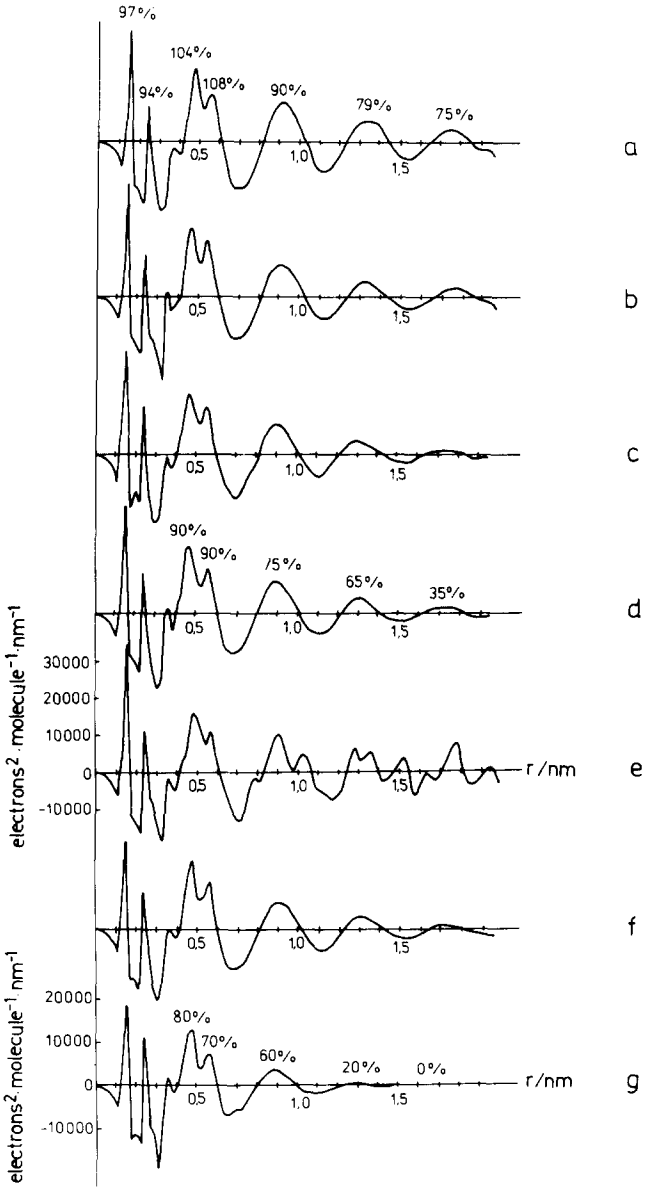

Figure 6 Reduced RDFs as obtained from $si(s)_{corr2}$ data for samples (a) 1, (b) 2, (c) 3, (d) 4, (e) 5, (f) 6 and (g) 8. (a) also contains the percentage ratios of the reduced RDF peak maximum heights of sample 1 to the corresponding data given in Reference 12; (d) gives the percentage ratios of the intermolecular reduced RDF maxima of samples 4 and 1; (g) contains the analogous percentage ratios of sample 8 to sample 6

species the following equation is valid for the determined reduced RDF:

$$(2r/\pi)\int_0^\infty si(s)\sin(rs)\,ds = 4\pi r^2 \sum_{i,j}^{m} K_i K_j p_{ij}(r) - 4\pi\rho_0 r^2\left(\sum_{i=1}^{m} Z_i\right)^2 \quad (9)$$

with Z_i and K_i the number of electrons and the mean effective number of electrons in atom i, respectively $(K_i(s) = f_i(s)/f_e(s)$, where $f_i(s)$ is the atomic scattering amplitude of atom i and $f_e(s)$ the mean scattering amplitude of an electron in the molecule). The $p_{ij}(r)$ are the atomic pair-correlation functions and m is the number of atoms in the molecule. With regard to the more complex solution systems discussed here the reduced

RDF is equal to the following sum:

$$4\pi r^2 \sum_{\substack{i,j=1 \\ i \neq j}}^{m} \omega_{(k)} K_i^{(k)} \omega_{(l)} K_j^{(l)} p_{ij}^{(k,l)}(r) - rA(r) \qquad (10)$$

ω_k is the mole fraction of species k ($k = 1$, H_2SO_4, $k = 2$, H_2O, $k = 3$, POD) and $\omega_{(k)} K_i^{(k)}$ means that K_i has to be multiplied by ω_k if the atom i is from molecular species k (H_2SO_4, H_2O or POD). $A(r)$ was defined in equation (4).

In *Figures 5a* and *6a* (100% H_2SO_4, sample 1) the percentage ratios of our reduced RDF peak maxima and the respective data obtained from the very careful investigation on pure H_2SO_4 of Weidner *et al.*[11,12] are also given. (Note that the intramolecular S–O and O–O maxima at 0.15 and 0.245 nm, respectively, were taken from an RDF for comparison.) Taking into consideration the limited resolution Δr of ≈ 0.021 nm, the coincidence of our data with the data of Weidner *et al.* is very good in the range $0 \leqslant r \leqslant 0.6$ nm, whereas our reduced RDFs are increasingly damped (e.g. to 70–75% for the peak at 1.74 nm) for increasing $r > 0.6$ nm in comparison to the literature data. The intensity deviations at large r are slightly greater for the reduced RDF data from $si(s)_{corr1}$ (*Figure 5a*) than for the respective data from $si(s)_{corr2}$ (*Figure 6a*). Significant deviations (≈ 0.05 nm) between the peak positions of our reduced RDFs and the respective functions in References 11 and 12 are present for $r > 1.1$ nm and $r > 1.5$ nm for the data given in *Figures 5a* and *6a*, respectively.

In spite of the slight differences between our reduced RDF data of the 100% H_2SO_4 standard sample and the best literature data on this material known to us[11,12], the following discussion is reasonable. There are no pronounced termination ripples in our reduced RDFs except for two subsidiary maxima around the peak at 0.15 nm in *Figure 5*, which are usually absent for fully corrected reduced RDFs (*Figure 6*).

The intramolecular RDF contains considerable contributions only for $r < 0.3$ nm even for 14 wt% POD content as can be seen from *Figure 7*. Therefore, the reduced RDFs for the POD solutions (see *Figures 5* and *6*) are of intermolecular nature for $r > 0.3$ nm to a very good approximation. Thus a serious overlap between the intra- and intermolecular parts of the reduced RDFs is then present only in the region of hydrogen bond distances ($r \approx 0.25$ nm).

The principal character of the reduced RDF curve of 100% H_2SO_4 remains nearly unchanged when 0–14 wt% POD is dissolved in this solvent. But in the concentration range 0–10 wt% POD a continuous decrease of intermolecular reduced RDF peak heights with increasing r can be noticed (see *Figures 6a–c*). In the 10–14 wt% POD range a further significant reduction of reduced RDF peak intensities is not found (see *Figures 6c,d*). Between 14 and 15 wt% POD concentration some of the material is involved in a phase transition from an isotropic solution to a crystal solvate (see References 6, 9 and 10) connected with considerable changes in the intermolecular distance distribution (see *Figure 6e*).

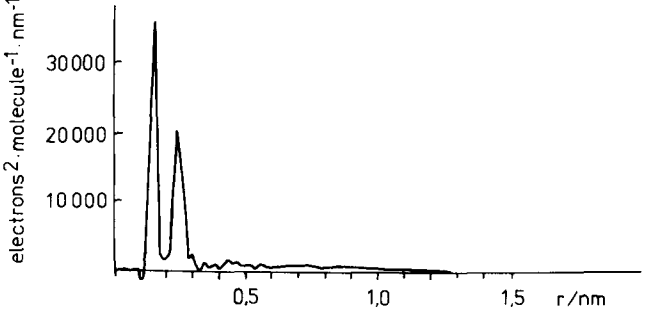

Figure 7 Intramolecular RDF for sample 4 calculated by using equation (8)

The percentage ratios of the intermolecular reduced RDF peak heights of the 14 wt% POD solution and the respective peak heights in the 100% H_2SO_4 curve (*Figure 6a*) are also given in *Figure 6d*. These ratios are measures for the short range interaction between the neighbourhood of an arbitrarily chosen H_2SO_4 molecule and the monomers of the POD molecules in comparison with the pure 100% H_2SO_4 solvent.

Weidner *et al.*[12] defined four correlation zones around an arbitrary H_2SO_4 molecule. Relatively strong orientation and distance correlations exist in the first zone ($0 < r < 0.48$ nm), whereas in the second zone ($0.48 < r < 1.0$ nm) reduced orientation and distance correlations are characteristic. In the third zone ($1.0 < r < 1.8$ nm) only a certain distance correlation occurs and in the fourth zone ($r > 1.8$ nm) preferential intermolecular distances cannot be found.

Only weak interactions (mainly solvation with protonation of POD monomer units at the oxygen atom[22], which results in a partial POD–H_2SO_4 solvation) occur if < 15 wt% POD is dissolved in 100% H_2SO_4, since the reduced intermolecular RDFs of these solutions show the same qualitative features as the respective function for the pure solvent. Therefore, the POD molecules are obviously nearly statistically distributed in the solvent. Thereby the first correlation zone of a representative H_2SO_4 molecule is less disturbed by the presence of POD than the second correlation zone and so on in comparison to the situation in the pure solvent. This perturbation of the pure H_2SO_4 correlation lattice increases with increasing POD concentration with certain saturation at 10 wt% POD content. (Note that all available dissociated H_2SO_4 ion pairs may be included in POD–H_2SO_4 solvation processes at ≈ 10% POD concentration.)

Between 14 and 15 wt% concentration of POD, the material undergoes a phase transition from the isotrope amorphous solution to crystal solvates plus isotropic solution of reduced POD concentration. Then the short-range interaction between monomeric units of POD and H_2SO_4 molecules in the crystal solvates cannot further be considered as a simple perturbation of the pure 100% H_2SO_4 correlation lattice. According to Milkova *et al.*[9] (see also References 6 and 10) the crystal solvate of POD in H_2SO_4 has the following unit cell parameters: $a = 1.175$, $b = 0.49$, $c = 1.465$ nm, $\alpha = 87.4$, $\beta = 86.4$, $\gamma = 90°$ with an H_2SO_4 molecule to POD monomer ratio of 1:1 in the crystalline lattice. This means that the H_2SO_4–POD interaction in a $\geqslant 15$ wt% (11 mol%) POD solution is strong enough to create local regions of increased POD concentration (50 mol% in the crystal solvate).

The 96.2 wt% H_2SO_4 solvent shows a reduced intermolecular RDF which is similar to the respective curve for the 100% H_2SO_4 but with a systematic decrease of peak intensities with increasing distances (see *Figures 5a*, *6a*, *5f* and *6f*). This result is consistent with other results in the literature on H_2SO_4 in the concentration range

90–100 wt%[23,24]. In the 96.2 wt (82.3 mol)% H_2SO_4 the correlation lattice which is present for 100% H_2SO_4 is obviously disturbed by short-range H_2O–H_2SO_4 interactions, e.g. in connection with H_2O protonation and H_2SO_4 self-protonation. These processes then lead to a reduction of the average correlation length. The considerable protonation and self-protonation processes in the 96.2 wt% H_2SO_4 may change the intramolecular distance distribution in comparison to the pure sulphuric acid (sample 1). Therefore, systematic errors could be present in this case in the intramolecular reduced intensity calculated by using equation (8). This could be the reason for some remarkable differences between the $si(s)_{corr1}$ and $si(s)_{corr2}$ curves for the 96.2 wt% H_2SO_4 solvent and the 6 wt% solution of POD in it (see *Figures 2c,d* and *4c,d*). But the following discussion of intermolecular reduced RDF peaks should be reasonable, because the difficulties in the choice of an appropriate molecular unit for equation (8) affects the intramolecular distance range only (see *Figures 5f,g* and *6f,g*).

A 0.5 wt% POD content in 96.2 wt% H_2SO_4 (sample 7) does not change the reduced RDF of the pure solvent significantly, whereas for the 6 wt% POD solution (sample 8) a very strong reduction of distance correlation compared with the pure solvent is observed (compare *Figure 6g* with the percentage ratios of the intermolecular RDF peak heights of sample 8 to the pure solvent sample 6). The interactions of the POD molecules with the correlation lattice of the 96.2 wt% H_2SO_4 solvent are clearly much stronger than for the same POD content in a 100% H_2SO_4 solvent (see *Figures 6b,d,g*). This is mainly due to the much higher degree of dissociation in 96.2 wt% aqueous H_2SO_4 than in pure sulphuric acid, which results in a considerably higher level of POD–H_2SO_4 solvation interaction in POD solution 8 than in solutions 2–4. A further discussion of this topic will be given in a subsequent publication[27].

CONCLUSIONS

Reduced RDFs for non-crystalline solutions of POD in H_2SO_4 have been discussed for the first time. A two-step correction procedure (first and second step according to References 16 and 11, respectively, with some modification in connection with the complex character of the investigated system) was performed for the correction of the reduced scattering intensities for systematic errors. Termination ripples in the reduced RDFs were minimized by using a special sampling procedure proposed by Lovell *et al.*[20].

The principal character of the reduced RDF of pure H_2SO_4 remained nearly unchanged when 0–14 wt% POD was dissolved in this solvent. But a continuous decrease of intermolecular reduced RDF peak maxima with increasing distance r and POD concentration was found. This was proposed to be the result of a simple perturbation of the short range correlation lattice of 100% H_2SO_4. Between 14 and 15 wt% POD content a phase transition from isotrope solution to crystal solvates plus isotrope solution of reduced POD content occurs.

The reduced RDF of a 96.2 wt (82.3 mol)% H_2SO_4 solvent resembles the reduced RDF of the 14 wt% solution of POD in 100% H_2SO_4. This is due to H_2SO_4–H_2O interactions (e.g. protonation). The interactions of the POD molecules with the short range correlation lattice of the 96.2 wt% H_2SO_4 solvent are considerably stronger than for the same POD content in a 100% H_2SO_4 solvent.

ACKNOWLEDGEMENT

We are greatly indebted to Dr E. Leibnitz for the synthesis of the POD used.

REFERENCES

1 Frazer, A. H. and Wallenberger, F. T. *J. Polym. Sci.* 1964, **A2**, 1171
2 Krutchinin, N. P., Romanov, W. W., Koschevnikov, J. P., Gatschinskaya, N. A., Semenova, A. S. and Kulichigin, W. G. *Chim. Vol.* 1983, **1**, 15
3 Kalashnik, A. T., Volokhina, A. V., Semenova, A. S., Kusnezova, L. K. and Papkov, S. P. *Chim. Vol.* 1977, **4**, 51
4 Bobrovnickaja, N. I., Romanov, V. V., Kalashnik, A. T., Sorokin, W. E., Semenova, A. S. and Makarova, R. A. *Chim. Vol.* 1983, **1**, 42
5 Eftimova, S. G., Okromchedlidse, N. P., Volokhina, A. V. and Iovleva, M. M. *Vysok. Soed.* 1977, **B19**, 67
6 Baird, D. G. and Silver, F. M. *J. Appl. Polym. Sci.* 1979, **23**, 941
7 Grebenkin, A. N., Antonov, N. G. and Kol'tsov, A. I. *Vysok. Soed.* 1989, **B31**, 203
8 Iovleva, M. M., Platonov, W. A., Okromchedlidse, N. P., Milkova, L. P. and Ivanova, N. A. *Vysok. Soed.* 1981, **B23**, 358
9 Milkova, L. P. and Poschalkin, N. S. Preprints of the 4th International Symposium on Man-made Fibres, Kalinin, USSR, 1986, Vol. 1, 236
10 Schelle, H., Hofmann, D. and Weigel, P. *Acta Polym.* 1989, **40**, 450
11 Weidner, J. U., Geisenfelder, H. and Zimmermann, H. *Ber. Bunsenges. Phys. Chem.* 1971, **75**, 800
12 Weidner, J. U., Geisenfelder, H. and Zimmermann, H. *Ber. Bunsenges. Phys. Chem.* 1972, **76**, 628
13 Pitkänen, T., Cooper, M. J., Laundry, D. and Holt, R. S. *Nucl. Instrum.* 1987, **A257**, 384
14 Pitkänen, T. Report Series in Physics, University of Helsinki, 1988, HU-P-248
15 Krogh-Moe, J. *Acta Cryst.* 1956, **9**, 951
16 Kaplow, R., Strong, S. L. and Averbach, B. L. *Phys. Rev.* 1965, **138**, A1336
17 Narten, A. H. and Levy, H. A. *J. Chem. Phys.* 1971, **55**, 2263
18 Popik, N. I., Shablygin, M. V., Vilkov, L. V., Semenova, A. S. and Kradchenko, T. V. *Vysok. Soed.* 1983, **B25**, 38
19 Brydon, D. L., Fisher, I. S., Emans, J., Smith, D. M. and MacDonald, W. A. *Polymer* 1989, **30**, 619
20 Lovell, R., Mitchell, G. R. and Windle, A. H. *Acta Cryst.* 1979, **A35**, 598
21 Kruh, R. F. *Chem. Rev.* 1962, **62**, 319
22 Volokhina, A. V., Braverman, L. P., Kudryavtsev, G. I., Okromchedlidze, N. P., Eftimova, S. G. and Papkov, S. P. *Chim. Vol.* 1974, **4**, 13
23 Finbak, C., Ronning, O. and Viervoll, H. *Tidskr. Kjemi Bergves. Metall.* 1944, **4**, 26
24 Shapovalov, I. M. and Radchenko, I. V. *Z. Strukt. Chim.* 1969, **10**, 921
25 'International Tables for X-Ray Crystallography', Vol. 4, Kynogh-Press, Birmingham, 1974
26 Hajdu, F. *Acta Cryst.* 1972, **A28**, 250